Development of strut-and-tie model and design guidelines for improved joint in decked bulb-tee bridge

Lungui Li[*1], Zhiqi He[2a], Zhongguo John Ma[3b] and Lingkan Yao[1c]

[1]*School of Civil Engineering, Southwest Jiaotong University, 111 Erhuan Rd. North 1 Section, Chengdu, 610031, China*
[2]*School of Civil Engineering, Southeast University, 2 Sipailou, Nanjing, 210096, China*
[3]*Department of Civil and Environmental Engineering, University of Tennessee Knoxville, 223 Perkins Hall, Knoxville, 37996-2010, USA*

Abstract. This paper focuses on a development of strut-and-tie model (STM) to predict the capacity of an improved longitudinal joint for decked bulb-tee bridge systems. Nine reinforced concrete beam/slab specimens anchored by spliced headed bars with different details were tested. Test results were evaluated and compared with an anticipation of the validated STM. The proposed STM provides a lower bound of the ultimate capacity of the joint zone. It shows that the lap length of headed bars has a significant effect on structural behaviors of the improved joint. To develop a full strength joint, the range of the lap length can be determined by the strength and compatibility requirement. Design recommendations to spliced headed bars, concrete strength, as well as lacer bars in the joint zone are proposed for developing a full strength joint.

Keywords: lap length; headed reinforcement; joint zone; strut-and-tie model; accelerated construction

1. Introduction

Considering the disruption of traffic and the cost of on-site labor, the rapid speed of bridge construction has become a more critical issue than ever before. The use of the decked bulb-tee (DBT) girder for the bridge superstructure by Stanton and Mattock (1986) is one of promising systems for accelerated bridge construction. The DBT girder includes a bridge deck precast and prestressed with a girder, manufactured in precast plants under closely monitored conditions, transported to construction sites, and erected such that flanges of adjacent units abut with each other. Load transfer between adjacent girders along bridge width direction is provided by longitudinal joints (parallel to traffic direction). Beside the longitudinal joint, a transverse joint (perpendicular to traffic direction) is used to connect ends of adjacent DBT girders over piers for multi-span bridge system. Fig. 1 shows a typical two-span bridge consisting of ten DBT girders connected by four longitudinal joints in each span as well as one transverse joint over the middle pier.

---

*Corresponding author, Associate Professor, E-mail: lgli@home.swjtu.edu.cn
[a]Assistant Professor
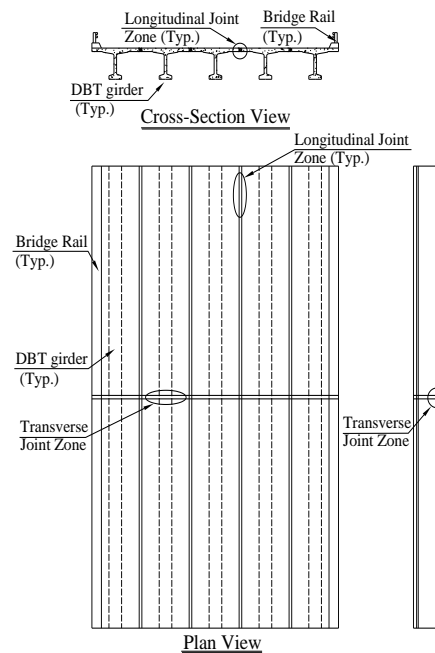[b]Associate Professor
[c]Professor

Fig. 1 A typical two-span DBT bridge connected by four longitudinal joints and one transverse joint
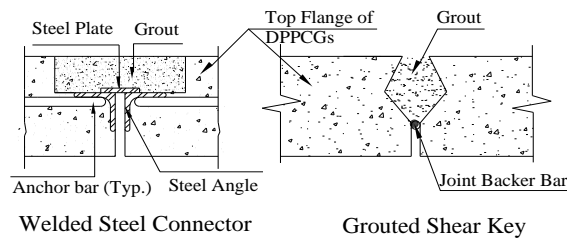

Fig. 2 Current joint details

This system eliminates the time necessary to form, place, and cure a concrete beam or deck at bridge sites. Currently, the joint zone consists of welded steel connectors and a grouted shear key (Stanton and Mattock 1986, Ma *et al.* 2007) shown in Fig. 2. This joint detail has the strength needed to transfer shear and limited moment from one girder to adjacent girders. The width of the joint zone is small so that it facilitates accelerated construction. However, since welded steel connectors are discontinuous and the spacing is from 1219mm (4 feet) to 2438mm (8 feet), they can not help to control flexural cracks well.

Huge amount of work has been done to improve current joint details for DBT system. The spirally confined straight lap splices of deformed reinforcing bars in concrete were researched (Einea *et al.* 1999). Parameters covered in this study include concrete strength, bar size, number of spirals, and lap length. The investigation showed that spiral confinement of lap splices of standard reinforcing bars can result in significant reduction of the required lap length, which facilitated the small width of the joint zone. However, workability of the joint pouring is a potential concern due to the much reinforcement placed in the joint. University of Tennessee Knoxville (Chapman 2010,
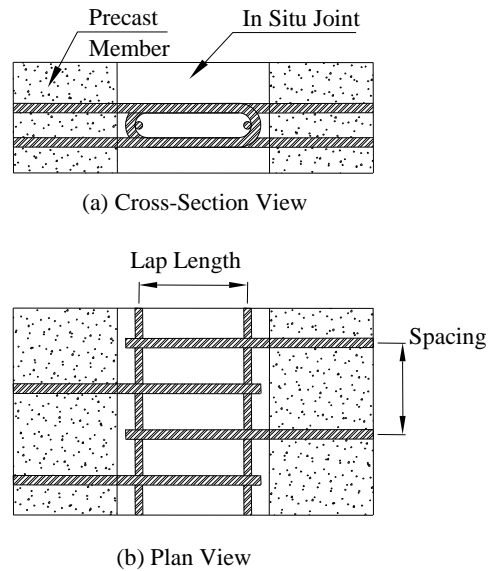
(a) Cross-Section View

(b) Plan View

Fig. 3 U bars anchoring joint

Zhu 2012, Ma 2012) explored 180 degree tight bend rebars (U bar) to provide continuity across the joint. The staggered reinforcement details provide both moment transfer and tension transfer over the joint, and the simple reinforcement layout facilitates the concrete or grout pouring in the joint. However, in order to minimize the thickness of the deck, the bend diameter of $3d_b$ is adopted. Based on the requirement of the minimum bend diameters established by American Concrete Institute (ACI Committee 318 2011), this tight bend diameter is smaller than what is required. Thus, deformed wire reinforcement (DWR) and stainless steel have to be used. Currently, the ACI318-11 code has not included the minimum bend diameter requirement for the special reinforcement. As an alternative, headed bar details are proposed in this paper.

To take advantage of DBT system with the feature of rapid construction, improved spliced headed bar joint details with accelerated construction feature were proposed and tested (Thompson 2006, Lewis 2009, Li 2010). These studies proposed design recommendations based on testing performance; however, the theoretical modeling which analyzes the mechanism of structural behaviors as well as design guidelines for the widespread application shall be needed. Based on testing, this paper focuses on a development of strut-and-tie model to analyze this type of joint subjected to flexural loads as well as tension loads. Design guidelines are further studied to facilitate the design of both longitudinal joints and transverse joints with spliced headed bar details.

2. Improved joint with spliced headed bar details

The desirable joint details shall have the following features. First, it should be a full strength joint to transfer internal forces such as moment, shear, and tension between girders, while the failure mode shall be ductile rather than brittle. Second, the width of the joint should be minimized to aid accelerated construction. University of Tennessee Knoxville (He *et al*. 2012) analyzed the structural behaviors and proposed the design guidelines for the joint anchored by the tight bend U bar based on
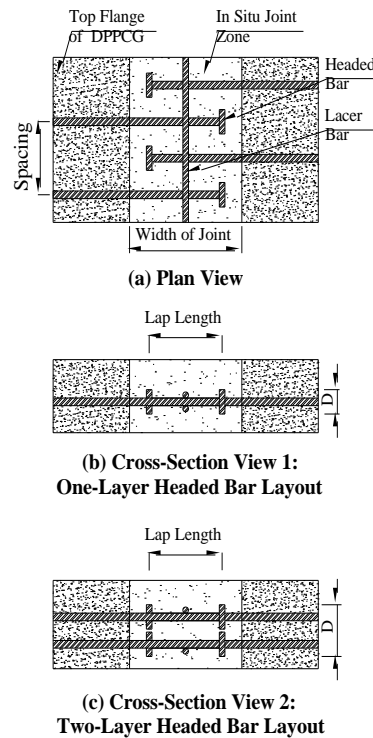
Fig. 4 Improved headed bar joint details

the strut-and-tie model. Fig. 3 shows the cross section view and plan view of the staggered U bars, which project from the adjacent precast members, anchoring the in situ joint. One lacer bar was placed through the end of the U bar on each side to provide reinforcement confinement along joint direction.

Specimens with different U bar spacing, lap length, reinforcement yielding strength as well as compressive strength of the in situ joint were tested. Strut-and-tie model was developed and verified by test programs. The strut-and-tie model proposed conservative strength predictions for the joint anchored by U bars. However, there are two concerns about the U bar anchorage. One concern is that the use of $3d_b$ bend diameter of the U bar is not applicable for the rebar except deformed wire reinforcement. Since the bend of the U bar requires enough room along the depth direction, another concern is that the U bar may not be used in the anchorage of the precast members with shallow depth.

Improved spliced headed bars joint details, which were applicable for different types of reinforcement as well as precast members with various depths, were proposed by the University of Tennessee Knoxville (Li *et al*. 2010). The improved joint details consist of distributed spliced headed bar in the in-situ joint zone shown in Fig. 4. The headed bars project from the top flange of DBT, and they are spliced with the headed bars in the adjacent precast members. The width of the joint is determined by the lap length of the headed bars, which is kept as small as possible to facilitate the accelerated construction. One lacer bar is placed above and below the spliced headed bars to provide the reinforcement confinement in the perpendicular direction. The grout shall be filled into the void of the joint to connect the adjacent girders. From the view of concrete protection for reinforcement,

51 mm (2 inches) of top cover and 25 mm (1 inch) of bottom cover shall be maintained based on the requirement by AASHTO LRFD (2010). There are two alternative headed bar details in cross-section view of the joint. One is the one-layer headed bar layout shown in Fig. 3(b) for the precast top flange with limited depth. Another is the two-layer headed bar layout shown in Fig. 3(c). The two-layer reinforcement details can be used in the precast members with enough rooms along depth's direction. For both layout details, the main variables are reinforcement lap length, spacing, yielding strength, and concrete compressive strength in the joint zone.

3. Summary of experimental programs

The tests were conducted to validate the performance of the improved joints with spliced headed bar details. Laboratory specimens consisted of five beam specimens with one-layer headed bar layout, two beam specimens with two-layer headed bar layout, as well as two slab specimens with one-layer headed bar layout. The joint zone was subjected to flexural loads, pure tension, and flexure-shear loads respectively.

3.1 Specimen dimension

A total of seven beam specimens and two slab specimens with variable dimensions or reinforcement details were fabricated. All specimens were designated according to the typical situation of DBT.

Fig. 5(a) shows the dimension of the five beam specimens (1H-B1, 1H-B2, 1H-B3, 1H-B4, and 1H-B5) with one-layer headed bar layout. All the five specimens were 610 mm (2 feet) wide, 3,048 mm (10 feet) long, and 152 mm (6 inch) deep. The variables in these specimens are the lap length of the headed bar, headed bar spacing, as well as the concrete compressive strength in the joint zone. Fig. 5(b) shows the dimension of the slab specimen with one-layer headed bar layout. Two slabs with the same dimensions were fabricated for flexure loading (1H-S1) and shear-bending load (1H-S2). The slab specimen consists of two panels. Each panel is 1829 mm (72 inch) wide, 1626 mm (64 inch) long, and 152 mm (6 inch) deep. The female-to-female shear key was provided at the vertical edge of both ends in the panel length direction, which connected the two panels as one slab. The lap length and spacing of the headed bar was 152 mm (6 inch). After the flexure test, the slab was cut along the joint zone. Then, the detached two panels were re-connected along the other edge to be fabricated the second slab. This allowed the panels can be used for the two slab tests. All the specimens shown in Fig. 5(a) and Fig. 5(b) had four layers of reinforcement both at the left side and the right side to simulate the deck reinforcement in the top flange of the precast girders. The headed bars spliced with the deck reinforcement long enough to avoid pulling out.

If two-layer headed bar layout is adopted, the depths of the precast top flange shall be increased accordingly to meet the requirement of the concrete cover as well as the reinforcement clearance. In order to keep the depths of the top flange as small due to the weight concern, the deck reinforcement was exploited as the spliced headed bar to reduce the room accommodating the additional bars. Fig. 5(c) shows the dimension of the beam specimens with two-layer headed bar layout (2H-B1). The outer deck reinforcement in bridge transverse direction was used as spliced headed bars in the longitudinal joint of the bridge. The specimen was 381 mm (1.25 feet) wide, 3,048 mm (10 feet) long, and 159 mm (6.25 inch) deep. The lap length and spacing of the headed bar was 152 mm (6 inch) and 114 mm (4.5 inch) respectively. Fig. 5(d) shows the dimension of the beam specimens
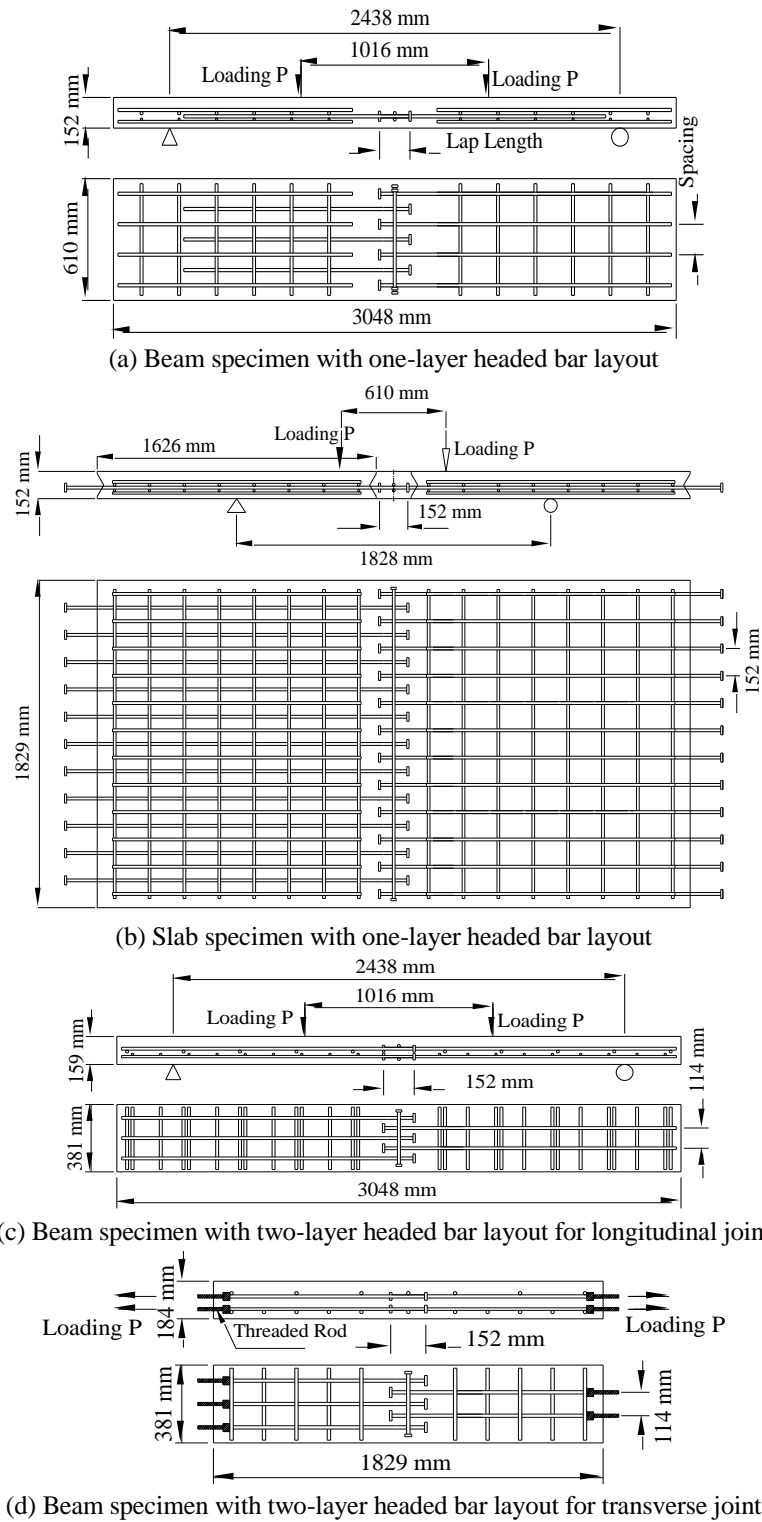
(a) Beam specimen with one-layer headed bar layout

(b) Slab specimen with one-layer headed bar layout

(c) Beam specimen with two-layer headed bar layout for longitudinal joint

(d) Beam specimen with two-layer headed bar layout for transverse joint

Fig. 5 Specimen dimension

Table 1 Main variables of specimens

Specimen	f'_c MPa	l mm	s mm
1H-B1	72.7	152	152
1H-B2	56.7	64	152
1H-B3	61.1	152	102
1H-B4	61.7	64	102
1H-B5	58.5	102	152
1H-S1	38.2	152	152
1H-S2	51.1	152	152
2H-B1	66.1	152	114
2H-B2	66.1	152	114

with two-layer headed bar layout (2H-B2) used in the transverse joint. Since the transverse joint locating over the piers to connect the ends of the adjacent precast girders, its direction is perpendicular to the direction of the longitudinal joint. The inner deck reinforcement along bridge traffic direction was used as the spliced headed bar in the transverse joint of the bridge. The specimen was 381 mm (1.25 feet) wide, 1,829 mm (6 feet) long, and 184 mm (7.25 inch) deep. The lap length and spacing of the headed bar was 152 mm (6 inch) and 114 mm (4.5 inch) respectively. In all the specimens shown in the Fig. 5, one headed reinforcement is placed above and below the spliced headed bar to simulate the lacer bar in the improved joint details (Fig. 4). All the spliced headed bar was grade 60 with diameter of 16 mm (#5 bar). The lacer bar was grade 60 with diameter of 13 mm (#4 bar). The diameter of the head is 51 mm (2 inch) and 38 mm (1.5 inch) for the one-layer headed bar and two-layer headed bar, respectively. The main variables of each specimen including concrete strength f'_c, headed bar lap length l, and spacing s were list in Table 1.

3.2 Instrumentation and test setup

To gain a better understanding of the behavior of the improved joint details, the spliced headed bar and the lacer bar were instrumented with strain gages. As shown in Fig. 6, the strain gages were place on the spliced headed bar in the joint zone, as well as at the middle and the quarter of the lacer bar.
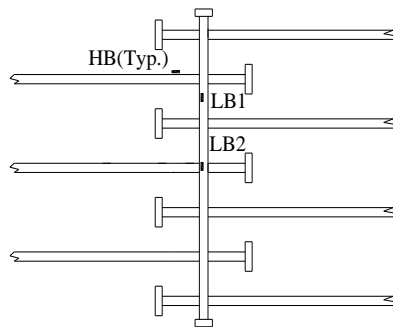

Fig. 6 Strain gage instrumentation

Fig. 7 Tension test setup

The longitudinal joint connecting the adjacent top flange of precast girders is a part of the bridge deck. Since the joint locates at the middle of the bridge deck between two adjacent girder webs, the flexural behavior is significant under the dead loading and vehicle loads. The specimens shown in Figs. 5(a), (b), and (c) representing the improved longitudinal joint details were tested in bending. All the specimens were simply supported. For the beam specimens with one-layer and two-layer headed bar layout (Figs. 5(a), (c)), the two *P* loadings were applied at the same value simultaneously and the joint zone has the pure flexural behavior. For slab specimen shown in Fig. 5(b), both the *P* loading on the left side of the joint zone (solid arrow) and the *P* loading on the right (hollow arrow) were applied on the specimen 1H-S1, where the joint zone experienced pure flexural behavior as beam specimens. However, only the *P* loading on the left side of the joint zone (solid arrow) was applied on the specimen 1H-S2, and the joint zone experienced flexural-shear behavior.

The transverse joint connects the ends of the adjacent precast girders over piers where are the negative moment regions under the dead loading and service loads. Because of the tensile forces created by the negative moment at the top of the bridge deck, the specimen shown in Fig. 5(d) representing the transverse joint were tested in tension. The ends of the headed bar in the specimen 2H-B2 were welded to the threaded rods. Then, these threaded rods were bolted to the support beam and the loading beam. The support beam on top of the loading frame was braced and clamped to remain stationary. The loading beam was connected to the actuators. The actuators pushed the loading beam down to apply the tension force to the specimen. Fig. 7 shows the tension test setup. A concern of the tension test was the strength of the welds between the end of headed bars and the threaded rods. If the welds were to fail before the specimen, the test would be invalid. The preliminary tension test was performed on the welding of headed bars and the threaded rods ensuring that the weld strengths were greater than the headed bar yielding strength.

Tension tests were performed on the grade 60 spliced headed bars in the joint zone, and the testing yielding strength is 467.4 MPa (67.5 ksi).

3.3 Test results

The testing results of moment capacity of specimens under flexural loading, and the tensile capacity (underlined value) of the specimen under tension loading were listed in Table 2. The

Table 2 Comparison of testing results and prediction

Specimen	Moment/<u>Tension</u> Capacity, kN-m / <u>kN</u>								$\dfrac{Test}{STM}$	$\dfrac{Test}{SA}$
	Test	Anticipation								
		SA	STM							
			T_{us}	T_{uh}	T_{ul}	T_u	M_u			
1H-B1	35	28	574	279	1281	279	25		1.39	1.25
1H-B2	24	27	230	279	534	230	21		1.14	0.89
1H-B3	53	40	603	465	3203	465	40		1.33	1.33
1H-B4	44	41	413	465	1334	413	36		1.21	1.07
1H-B5	25	27	369	279	854	279	25		1.00	0.93
1H-S1	99	89	1100	1024	4697	1024	87		1.13	1.11
1H-S2	91	91	1477	1024	4697	1024	89		1.02	1
2H-B1	39	30	465	372	2277	372	31		1.27	1.3
2H-B2	<u>400</u>	<u>372</u>	571	372	2277	372			<u>1.07</u>	<u>1.07</u>

Note: 1. SA is the notation of sectional analysis
2. The underlined numbers refer to the <u>Tension</u>

sectional analysis (Bentz and Collins 2000) was conducted to predict the moment capacity of the corresponding specimens with equivalent continuous reinforcement in the joint zone. For the specimen 2H-B2 under pure tension loading, the tension capacity was predicted by the tested yielding strength of four #5 bars without the contribution of the concrete for conservative purpose. The anticipated capacity of each specimen was shown in Table 2. The testing bend capacity of all flexural specimens with 152 mm lap length and variable spacing (152 mm, 114 mm, and 102 mm) of headed bar details (1H-B1, 1H-B3, 1H-S1, 1H-S2, 2H-B1) were larger than the anticipated values of specimens with equivalent continuous reinforcement by Bentz. The actual bend capacities of specimen 1H-B2 and 1H-B5 with the shorter lap length (64 mm, 102 mm) and 152 mm spacing were less than the predicted moment capacity. The ratio of the testing value and the Bentz anticipation for specimens 1H-B2 and 1H-B5 is 0.89 and 0.93 respectively. When the headed bar spacing reduced to 102 mm (4 inch), the specimen 1H-B4 with the lap length as short as 64 mm (2.5 inch) can provide considerable anchorage capacity, and the ratio of the testing value and the Bentz anticipation is 1.07. Taking the assumption of spliced headed bars as the equivalent continuous reinforcement, the sectional analysis can not reveal the mechanism of the force flow in the joint zone anchored by the spliced headed bar, nor it can predict the conservative capacity of the specimen with different joint details.

Flexural specimens exhibited two different behaviors under failure loading. Fig. 8(a) shows the typical ductile failure mode for specimen 1H-B1, 1H-B3, 1H-S1, 1H-S2 and 2H-B1. Flexural cracks were well-distributed along the tension side of the moment zone. The concrete on the compression side of the moment zone crushed when the failure load was reached. Fig. 8(b) shows the typical brittle failure mode for specimen 1H-B2, 1H-B4 and 1H-B5. There were not much distributed cracks in the moment zone. Near failure loading, one wide diagonal crack was developed and propagated over the joint zone. However, the top concrete was fairly good until failure. Fig. 8(c) shows the failure mode for tension specimen 2H-B2. The first cracks were transverse cracks evenly spaced along the length of the specimen. Additional loading produced longitudinal cracks above the headed reinforcement. When approaching the tension capacity of the specimen, diagonal cracks

(a) Ductile failure for flexural specimen
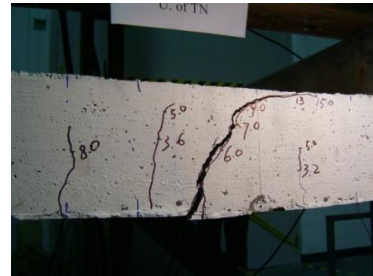
(b) Brittle failure for flexural specimen

(c) Tension specimen failure mode
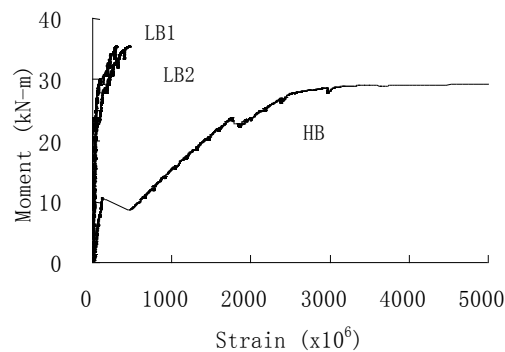
Fig. 8 Failure modes

Fig. 9 Headed reinforcement strain

appeared close to the sides of the specimens. The diagonal cracks propagated toward the transverse crack in the joint zone and caused the failure of the specimens.

The results from the strain gauge readings were plotted against the corresponding moment for flexural specimens. As shown in Fig. 9, the strain of the spliced headed bars in the joint zone (HB) well yielded at ultimate loading, while the strain at middle (LB2) and quarter (LB1) of the lacer bar was relatively small.

4. Strut-and-tie model

From the above study, it found that the sectional analysis considering the reinforcement as continuous bars can not reveal the force mechanism or provide the conservative capacity of the

improved joint connected by the spliced headed bars. The main parameters of the improved joint details shown in Fig. 3 are lap length of the headed bar l, spacing of the headed bar s, yielding strength of the headed bar f_{yh} and lacer bar f_{yl}, as well as the concrete compressive strength f'_c in the joint zone.

Since headed bars are staggered and they are not continuous in the joint, the joint zone cannot be analyzed by the conventional beam sectional method. The load transfer in the joint is related to the interaction between the distributed bars and the surrounding concrete. The strut-and–tie model is a detailing and ultimate strength method for discontinuity regions in reinforced concrete structures.

4.1 Strut and tie model for joint zone

The reinforced concrete structures can be divided into two regions: one is B-region where beam sectional theory is valid with assumption that strain varies linearly through the depth of member, and the other is D-region where discontinuities affect member behavior. The strut-and–tie model is an ultimate strength calculation method for D-regions in reinforced concrete structures. It represents the internal forces using a statically determinate truss and produces a safe solution. It origins from the flow of forces in structural concrete members presented around 1900s (Ritter 1899, Morsch 1909). Evolved in 1980s and 1990s (Marti 1985, Schlaich and Schafer 1991), the strut-and-tie model has been implemented into several codes and specifications (AASHTO LRFD 2010, ACI Committee 318 2008). The strut-and-tie model has been used to analyze the ultimate strength of the reinforced concrete members under different loading cases including torsion, bending, and shear (Mueller 1976, 1979).

The strut-and-tie model has three component: strut (internal compression member), tie (internal tension member), and nodal zone (points where the axes of struts, ties, or concentrated loads intersect). The improved joint shown in Fig. 4 is reinforced by the spliced headed bar where the internal forces supposed to be transferred between the opposite headed bars, lacer bars, and the surrounding concrete. The force transfer mechanisms in this region can be idealized by the strut-and-tie model represented by the right angled triangles (such as ABC) shown in Fig. 10. The headed bars and lacer bar are the tie members represented by solid line which take internal tension force (T). The concrete between two opposite spliced headed bars is the strut member represented by dash line resisting compression force (C). The head of the bar provides enough anchorage in the nodal zone. The compression force and the tension force are balanced at the node, so the improved joint detail is the C-C-T node. The angle between the axle of the strut and the axle of the tie is θ. Since the both lacer bars are placed in the middle of the spliced headed bar joint details and serve as the tie member (Fig. 4), there will be equal numbers of right angled triangle (strut-and-tie model) on each side of the lacer bar. All the strut-and-tie models in the joint zone are self-balanced between two adjacent models. Tie AB, strut AC and AD are balanced at node A for strut-and-tie model ABC and ABD. Tie BC and CE, strut AC and CF are balanced at node C for strut-and-tie model ABC and CEF.

4.2 Equations for force balance in strut-and-tie model

The load capacity of each member of the strut-and-tie model (such as model ABC) is controlled by the crushing of the diagonal concrete strut AC, the yielding of the headed bar AB and the lacer bar BC. The tension forces in the member of the lacer bar for all strut-and-tie models are equal
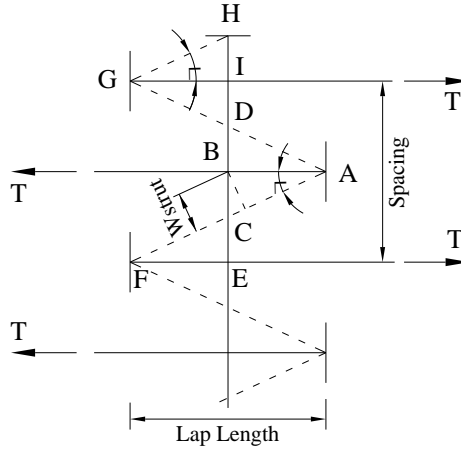
Fig. 10 Strut-and-tie model for joint zone

because the lacer bar member is the same rebar. The idealized failure mode of the joint zone is the crushing of the concrete AC and the yielding of the lacer bar BC after the yielding of the headed bar AB. Otherwise, the capacity of the headed bar cannot be obtained, and the ultimate load of the joint will be controlled by the concrete crushing or yielding of the lacer bar.

From force equilibrium, the internal force of each member in the strut-and-tie model (such as the right angled triangle ABC) can be expressed by

$$F_s = \frac{T}{2\cos\theta} \tag{1}$$

$$F_h = T \tag{2}$$

$$F_l = \frac{T}{2}\tan\theta \tag{3}$$

Where T is the tensile force applied on a headed bar; F_s, F_h, F_l are the internal forces in the concrete strut, headed bar, and lacer bar respectively; θ is the angle between the diagonal strut and the headed bar, which is determined in terms of the headed bar lap length l and the spacing s by the expression of $\cos\theta = \dfrac{2l}{\sqrt{4l^2 + s^2}}$.

According to ACI 2008, the ultimate strength of the strut and tie are specified as following

$$F_s = 0.85 f_c' A_{strut} \tag{4}$$

$$F_t = A_t f_y \tag{5}$$

Where: f_c' = compressive strength of concrete

A_{strut} = cross sectional area of a strut

F_t = nominal strength of a tie

A_t = cross sectional area of tie

f_y = yielding strength of reinforcement

Substituting the Eqs. (4) and (5) (ultimate strength of strut and tie) into Eqs. (1) to (3), the ultimate tension strength of a right triangle controlled by each strut or tie are expressed as

$$T_{us} = 2F_s \cos\theta = \frac{3.4 f_c' A_{strut} l}{\sqrt{4l^2 + s^2}} \tag{6}$$

$$T_{uh} = f_{yh} A_h \tag{7}$$

$$T_{ul} = \frac{2 f_{yl} A_l}{\tan\theta} = \frac{4 f_{yl} A_l l}{s} \tag{8}$$

where T_{us}, T_{uh}, T_{ul} are the ultimate tension capacity of a right angled triangle controlled by strut, headed bar, and lacer bar respectively; A_h and A_l are the area of the reinforcement for the headed bar and lacer bar respectively; f_{yh} and f_{yl} are the yielding strength of the headed bar and lacer bar respectively. The cross-sectional area of the diagonal strut A_{strut} is determined by

$$A_{strut} = DW_{strut} = \frac{Dl \sin\theta}{2} \tag{9}$$

where D is the depth of the diagonal strut, which equals to the diameter of the head for one-layer headed bar layout, or is the distance between the extreme outer edge of the head for two-layer headed bar layout as shown in Fig. 4. W_{strut} is the width of the diagonal strut shown in Fig. 10, which is calculated as the determination of the diagonal strut width in the truss model for a reinforced concrete beam (Collins and Mitchell 1991).

For the specimen anchored by N headed bars on one side (minimum number of the either side), the ultimate tension capacity T_u can be determined by

$$T_u = N \times \min(T_{us}, T_{uh}, T_{ul}) \tag{10}$$

The Eq. (10) can be further expressed as

$$T_u = N \times \min(\frac{1.7 f_c' Dl^2 s}{4l^2 + s^2}, f_{yh} A_h, \frac{4 f_{yl} A_l l}{s}) \tag{11}$$

4.3 Equations for moment capacity in joint zone

Eq. (11) estimates the tension capacity of the spliced headed bar with surrounding concrete in the strut-and tie model. However, for the longitudinal joint where the flexure behavior is significant, the moment capacity can be estimated by the sectional force equilibrium. The ultimate compression force C_u in the top zone of the longitudinal joint is equal to the tension force T_u in the bottom zone of the joint. Since the stress limit of $0.85 f_c'$ is imposed to the compression zone when the failure of the concrete occurs, the depth of the neutral axis c can be obtained by

$$c = \frac{C_u}{0.85 f_c' b} = \frac{T_u}{0.85 f_c' b} \qquad (12)$$

So, the ultimate moment capacity of the longitudinal joint can be estimated by

$$M_u = T_u \left(d_s - \frac{c}{2} \right) = T_u \left(d_s - \frac{T_u}{1.7 f_c' b} \right) \qquad (13)$$

where b is the width of the specimen, and d_s is the distance from the extreme compressive fiber to the centroid of the reinforcement. For the one-layer headed bar layout, the centroid of the reinforcement is the centroid of the headed bar. While for the two-layer headed bar layout, it is assumed that both layers of reinforcement yield and the location of the resultant tensile force coincides with the center of the two layers. It is noted that Eq. (13) is only good in the case of all the headed bars locate in the tensile zone of the section and yield at the failure of the joint.

4.4 Comparisons with testing

Table 2 lists the predicted T_{us}, T_{uh}, T_{ul}, T_u and M_u for each specimen according to Eqs. (11)-(13) based on the strut-and-tie modeling. It shows that the anticipated ultimate capacities of flexural specimens and the tension specimen by STM match with the experimental values well. The average value and the standard deviation of $\frac{Test}{STM}$ for the 9 flexural specimens is 1.19 and 0.14 respectively, while the value of $\frac{Test}{STM}$ for the tension specimen is 1.07. The proposed strut-and-tie method is a rational analysis method for discontinuous region based on strength capacity, and it provides safe and conservative predictions. From Table 2, it can been seen that the tension capacities controlled by the strength of the lacer bar T_{ul} are much larger than the values controlled by the strength of the headed bar T_{uh} and concrete strut T_{us} for all the testing specimens. The lacer bars were far away to the yielding when the specimens failed, which is in accordance with the small strain obtained on the lacer bar during the testing. The specimen 1H-B1, 1H-B3, 1H-S1, 1H-S2, 2H-B1, and 2H-B2 with 152 mm (6 inch) lap length and variable spacing have full strength joint where the spliced headed bars (tie) are well yielded before the concrete (strut) crushing based on the STM prediction (T_{us} is larger than T_{uh}). Until failure, there were lots of well distributed cracks in the joint zone, and the concrete in the top compression zone was crushed (for flexural specimen 1H-B1, 1H-B3, 1H-S1, 1H-S2 and 2H-B1) as shown in Fig. 8(a). The tension specimen 2H-B2 had numerous transverse cracks in the joint zone, and there was a large longitudinal crack propagating along the heads of the spliced headed bar as shown in Fig. 8(c).

For specimens 1H-B2 and 1H-B4 with 64 mm (2.5 inch) lap length, the spliced headed bars (tie) were not yielded yet until the crushing of the concrete (strut) based on the STM prediction (T_{uh} is larger than T_{us}). It indicates that the capacities of the specimens 1H-B2 and 1H-B4 are controlled by the concrete strength in the joint zone. The concrete in the top compression zone was still in good shape at failure, and there was a large diagonal crack propagating cross the joint when the specimen can not carry any more loadings as shown in Fig. 8(b). Specimen 1H-B5 has 102 mm (4 inch) lap length with 152 mm (6 inch) spacing, and the spliced headed bars (tie) were barely yielded when the concrete (strut) crushed. All the three specimens 1H-B2, 1H-B4 and 1H-B5 experienced the brittle failure and the deformation is small.

5. Design recommendations

From the testing results as well as the Eqs. (11) and (13), it can be observed that the capacity of the joint zone anchored by the spliced headed bar is determined by the following main parameters: concrete compressive strength, the relationship of the headed bar lap length and spacing, yielding strength of the reinforcement, and the area of the headed bar. Generally, the higher of the concrete compressive strength, the longer of the headed bar's lap length, and the more appropriate relationship of the headed bar lap length and spacing will produce the larger loading capacity of the joint. However, if the spacing is too small with certain lap length, the angle between the axle of the strut and tie is small. It will result in the incompatibility of the reinforcement and surrounding concrete because of the shorting of the strut and the lengthening of the tie occurring in almost the same direction.

The strategy of the joint design for precast members is to provide full strength, ductility as well as fast construction joint to meet the requirements of possible loading states. This paper focuses on the development of the full strength joint with proper details. To satisfy the strength and ductility, yielding of the headed bar shall be achieved before concrete crushing and yielding of the lacer bar. To satisfy the fast construction, the lap length shall be as narrow as possible.

5.1 Design of headed bar

The ultimate tension capacity controlled by the concrete strut T_{us} can be rearranged based on the Eq. (11)

$$T_{us} = \frac{1.7 f_c' D l^2 s}{4 l^2 + s^2} = 0.425 f_c' D l \sin(2\theta) \tag{14}$$

It can be seen that the strut capacity is increased proportional to the increasing of the concrete strength, depth of the strut, and the lap length of the headed bars. It reaches the maximum value when the angle between the axle of the concrete strut and the axle of the tie (headed bar or lacer bar) is equal to 45°, i.e., the lap length of the spliced headed bar is exact the half of the headed bars' spacing.

To develop a full strength joint, the tension capacity controlled by the concrete strut crushing should be greater than the one controlled by headed bar yielding, which has $T_{us} \geq T_{uh}$. Substituting Eq. (11) into the above inequality, it can be expressed by

$$l \geq \sqrt{\frac{f_{yh} A_h^2 s}{1.7 f_c' s D - 4 f_{yh} A_h}} \tag{15}$$

The angle θ between the axes of strut and tie shall not be taken as less than 25° (ACI 2008). Based on the above requirement, the angle θ between the axle of the strut (the dashed line) and the axle of the spliced headed bar (the continuous line) shown in Fig. 10 shall be between 25° to 65°.

Fig. 11 facilitates the database of the headed bar lap length range selection in the design of the typical joint anchored with one-layer 16 mm diameter (#5 bar) headed bar and 51 mm (2 inch) diameter head. The yielding strength of the headed bar is 467.4 MPa (67.5 ksi), and the concrete compressive strength is 48 MPa (7 ksi). The spacing of the headed bar is variable and it can be designed in accordance with the deck reinforcement in the precast girder. The lower bound (curved
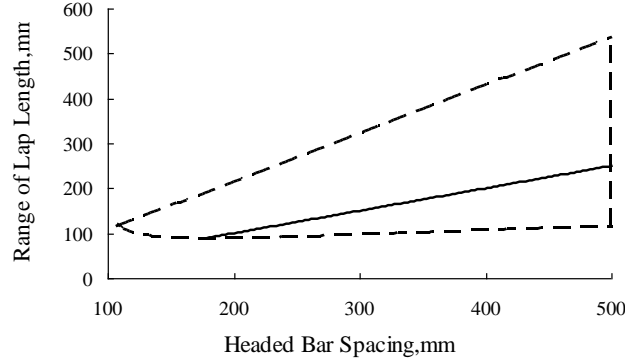
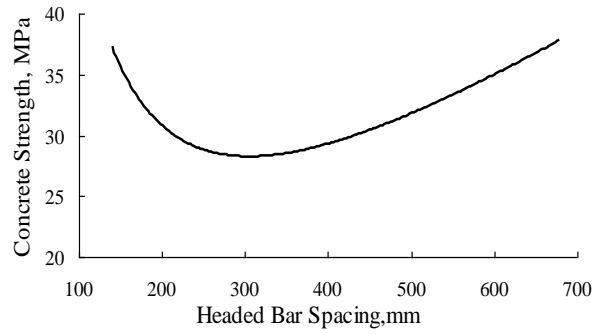Fig. 11 Lap length range of headed bars with spacing

Fig. 12 Required concrete strength with headed bar's spacing

dash line) is determined by Eq. (15), which ensures the yielding of the spliced headed bar before the crushing of the concrete strut. The minimum value, the maximum value of the headed bar spacing, and the upper bound (straight dash line) is set due to the angle θ shall be between 25° to 65°. The straight continuous line represents the status of the maximum strut capacity when the lap length is half of the spacing of the headed bar. The lap length of the spliced headed bar can be selected in the range of the dashed line, and it is optimized by the continuous line with the maximum concrete strut capacity. For the joint with different concrete strength and spliced headed bar details (yielding strength or area of rebar), the lap length range of headed bars with certain spacing can be determined accordingly.

5.2 Design of concrete strength in joint

To insure the full strength joint, which is $T_{us} \geq T_{uh}$, the concrete compressive strength should satisfy the following inequality based on the Eq. (11).

$$f_c' \geq \frac{f_{yh} A_h (4 + \frac{s^2}{l^2})}{1.7sD} \tag{16}$$

The Eq. (16) is plotted in Fig. 12 to propose the lower bound of the concrete strength in the joint based on the force equilibrium of the strut-and-tie model.

The lap length l is determined by the development length of the headed bar and should be as small as possible to facilitate the rapid construction. 152 mm (6 inch) was selected as the lap length, and the reinforcement details in the joint are one-layer 16 mm spliced headed bar (#5 bar) with 51 mm (2 inch) diameter head. The yielding strength of the headed bar is 467.4 MPa (67.5 ksi). The range of the headed bar spacing was determined between 100 mm to 700 mm based on the angle θ between 25° to 65°. The curve shows that, with certain lap length of headed bar, the required concrete strength decreases with the increasing of the spacing. When the headed bar spacing was twice as long as the lap length, where the angle θ between the axle of the strut and the axle of the tie was 45°, the required concrete strength in the joint reaches its minimum value. With the increasing of the angle θ beyond 45°, or further increasing of the headed bar's spacing, the required concrete strength increases accordingly. Please note that the concrete strength curve shown in Fig. 12 is the lower bound of the concrete strength required by the force equilibrium of the strut and tie interaction. To satisfy the structural performance of the cast-in-place joint with the precast members as well as the ductility, the designed concrete strength in the joint shall not be less than the one of the precast members and the calculated conservative values.

5.3 Design of lacer bars

The installing of adequate lacer bars along the longitudinal direction of the joint is necessary to prevent the crack along the transverse direction induced by concrete shrinkage, temperature change, as well as premature failure of the concrete core due to local splitting. In addition, the lacer bars need to have sufficient strength to balance the local stress from the compressive concrete strut based on the strut-and-tie model. Based on the Eq. (11), the tension capacity of the lacer bar and the spliced headed bar shall satisfy the following relationship to develop the full strength joint making sure the yielding of the headed bar before the yielding of the lacer bar.

$$\frac{f_{yl}A_l}{f_{yh}A_h} \geq \frac{s}{4l} \tag{17}$$

For conservative purpose and simplicity, $s/4l$ is taken as its maximum value of 1.07 based on the maximum angle θ of 65°. Taking one-layer spliced headed bar with 16 mm diameter (#5 bar), if the yielding strength of the lacer bar is the same as that of the headed bar, one lacer bar with 13 mm diameter (#4 bar) shall be placed above and under the spliced headed bar respectively.

6. Conclusions

Based on the analysis and comparison of strut-and-tie model and experimental programs of proposed spliced headed bar details, following conclusions are made:
  • The strut-and-tie model can provide a conservative strength anticipation of the joint anchored by spliced headed bars. The prediction is based on the internal force equilibrium, and it is the lower bound of the ultimate capacity of the joint zone.
  • The lap length of the headed bar has a significant effect on structural behaviors of the joint zone. It is a function of following variables: tension capacity and spacing of the headed bar, depth of strut, as well as the concrete strength. In order to develop a full strength joint, the range of the lap length can be determined by the strength requirement (yielding of the headed bar before the

crushing of the concrete) and the compatibility requirement (the angle between the axle of the strut and tie θ shall not less than 25°).

• The strut-and-tie model shows that the strut capacity is determined by the function of the lap length and spacing of the headed bar. It reaches its maximum value when the headed bar's spacing is twice as long as the lap length.

• To develop the full strength joint with ductile failure mode, spliced headed bars, concrete strength and lacer bars shall be properly designed as Eqs. (15), (16) and (17) respectively.

7. Future Work

Load transfer paths produced by the strut-and-tie model are not unique. For the improved joint, an alternative loading path exists since lacer bars are placed along the middle of the spliced headed bars. Topology approach will be emerged into strut-and-tie model to optimize possible load transfer paths by considering different arrangement of reinforcement, properties of the reinforcement and the concrete in the joint zone.

Acknowledgments

References

AASHTO LRFD (2010), Bridge Design Specifications, 5th Edition, American Association for State Highway and Transportation Officials, Washington, D.C.

ACI Committee 318 (2011), Building Code Requirements for Structural Concrete (ACI 318-11) and Commentary, American Concrete Institute, Farmington Hills, MI.

Bentz, E.C. and Collins, M.P. (2000), *Response-2000 Reinforced Concrete Sectional Analysis*. A software downloaded http://www.ecf.utoronto.ca/~bentz/r2k.htm.

Chapman, C.E. (2010), "Behavior of precast bridge deck joints with small bend diameter U-bars", Master Theses at University of Tennessee Knoxville.

Collins, M.P. and Mitchell, D. (1991), *Prestressed Concrete Structures*, Prentice Hall, 10 Englewood Cliffs, NJ.

Einea, A., Yehia, S. and Tadros, M.K. (1999), "Lap splices in confined concrete", *ACI Structural Journal*, **96**(6), 947-956.

He, Z., Ma, Z., Chapman, C.E. and Liu, Z. (2012), "Longitudinal joints with accelerated construction features in decked bulb-tee girder bridges: strut-and-tie model and design guidelines", *ASCE Journal of Bridge Engineering*, **18**(5), 372-379.

Lewis, S. (2009), "Experimental investigation of precast bridge deck joints with U-bar and headed bar joint details", Master theses at University of Tennessee Knoxville.

Li, L., Ma, Z., Griffey, M.E. and Oesterle, R.G. (2010), "Improved longitudinal joint details in decked bulb tees for accelerated bridge construction: concept development", *ASCE Journal of Bridge Engineering*, **15**(3), 327-336.

Li, L., Ma, Z. and Oesterle, R.G. (2010), "Improved longitudinal joint details in decked bulb tees for accelerated bridge construction: fatigue evaluation", *ASCE Journal of Bridge Engineering*, **15**(5), 511-522.

Ma, Z., Chaudhury, S., Millam, J.L. and Hulsey, L. (2007), "Field test and 3D FE modeling of decked bulb-tee bridges", *ASCE Journal of Bridge Engineering*, **12**(3), 306-314.

Ma, Z., Lewis, S., Cao, Q., He, Z., Burdette, E.G. and French, C.E.W. (2012), "Transverse joint details with tight bend diameter U-bars for accelerated bridge construction", *ASCE Journal of Structural Engineering*, **138**(6), 697-707.

Ma, Z**.,** Cao, Q., Chapman, C., Burdette, E. and French, C. (2012), "Longitudinal joint details with tight bend diameter U-bars", *ACI Structural Journal*, **109**(6), 815-824.

Marti, P. (1985), "Basic tools for reinforced concrete design", *ACI Journal*, **82**(1), 46-56.

Morsch, E. (1909), *Concrete-Steel Construction*, Trans. Goodrich, E.P., Mcgraw-Hill, New York.

Mueller, P. (1976), *Failure Mechanisms for Reinforced Concrete Beams in Torsion and Bending*, IABSE, V. 36-II.

Mueller, P. (1979), "Plastic Analysis of Torsion and Shear in Reinforced Concrete", Final Report, IABSE Colloquium on Plasticity in Reinforced Concrete, Copenhagen, May.

Ritter, W. (1899), "Die bauweise hennebique", *Schweizerische Bauzeitung*, **33**(7), 59-61.

Schlaich, J. and Schafer, K. (1991), "Design and detailing of structural concrete using strut-and-tie models", *The Structure Engineer*, **69**(6), 113-125.

Stanton, J. and Mattock, A.H. (1986), "Load distribution and connection design for precast stemmed multibeam bridge superstructures", NCHRP Rep. 287.

Thompson, M.K., Jirsa, J.O. and Breen, J.E. (2006), "Behavior and capacity of headed reinforcement", *ACI Struct. J.*, **103**(4), 522-530.

Zhu, P., Ma, Z**.,** Cao, Q. and French, C. (2012), "Fatigue evaluation of transverse U-bar joint details for accelerated bridge construction", *ASCE Journal of Bridge Engineering*, 17(2), 191-200.